A new Meckel's cartilage from the Devonian Hangenberg black shale in Morocco and its position in chondrichthyan jaw morphospace

Merle Greif[1], Humberto G. Ferrón[2], Christian Klug[1]

[1] Palaeontological Institute and Museum, University Zurich, 8006, Zurich, Switzerland.
[2] Instituto Cavanilles de Biodiversidad i Biología Evolutiva, Universitat de València, C/ Catedrático José Beltrán Martínez, 2, 46980 Paterna, Valencia, Spain; School of Earth Sciences, University of Bristol, Life Sciences Building, Bristol BS8 1TH, UK.

Corresponding Author:
Merle Greif[1]
University Zurich, Karl-Schmid-Strasse 4, 8006, Zurich, Switzerland.
Email address: merle.greif@pim.uzh.ch

Abstract

Fossil chondrichthyan remains are mostly known from their teeth, scales or fin spines only, whereas their cartilaginous endoskeletons require exceptional preservational conditions to become fossilized. While most cartilaginous remains of Famennian (Late Devonian) chondrichthyans were found in older layers of the eastern Anti-Atlas, such fossils were unknown from the Hangenberg black shale (HBS) and only a few chondrichthyan teeth had been found therein previously. Here, we describe a Meckel's cartilage from the Hangenberg black shale in Morocco, which is the first fossil cartilage from these strata. Since no teeth or other skeletal elements have been found in articulation, we used elliptical Fourier (EFA), principal component (PCA), and hierarchical cluster (HCA) analyses to morphologically compare it with 41 chondrichthyan taxa of different size and age and to evaluate its possible systematic affiliation. PCA and HCA position the new specimen closest to some acanthodian and

31 elasmobranch jaws. Accordingly, a holocephalan origin was excluded. The jaw shape

32 as well as the presence of a polygonal pattern, typical for tessellated calcified cartilage,

33 suggest a ctenacanth origin and we assigned the new HBS Meckel's cartilage to the

34 order Ctenacanthiformes with reservations.

36 **Introduction**

37

38 Fossil chondrichthyans (sharks, rays and chimaeroids) are mainly known from the

39 Devonian onward (Brazeau & Friedman 2015). Exceptional, putative chondrichthyan, as

40 well as acanthodian finds date back to the Silurian (Burrow & Rudkin 2014; Andreev et

41 al. 2016). Only teeth, scales and fin spines of chondrichthyans (whole group, including

42 acanthodians) are strongly mineralized while chondrichthyan endoskeletons are

43 predominantly made of unmineralized cartilage that is only rarely preserved (Seidel et

44 al. 2020).

45 Despite the difficulties of preservation, chondrichthyan skeletons are frequently found in

46 the middle and late Famennian strata in the Tafilalt and Maïder regions of southern

47 Morocco and constitute important contributions to the understanding of early vertebrates

48 (Ginter et al. 2002; Derycke et al. 2008; Frey et al. 2018; Frey et al. 2020). However, in

49 the late Famennian Hangenberg black shale layers of Morocco, nearly no vertebrate

50 remains have been collected or described so far. The only known contributions to the

51 vertebrate fossil record that are known from these strata are a few chondrichthyan

52 teeth, which are not described but only mentioned in the literature (Klug et al 2016; Frey

53 et al. 2018) as well as some chondrichthyan ichnofossils from layers just above the

54 Hangenberg black shale (basal Hangenberg Sandstone; Klug et al 2021). Here, we

55 describe a lower jaw found in the Anti-Atlas that represents the first reported

56 cartilaginous remain from the Moroccan Hangenberg black shale.

57 Outcrops of sediments that were laid down in the time around the end-Devonian

58 Hangenberg crisis can be found at many localities of the Tafilalt and Maïder regions of

59 the Anti-Atlas (Kaiser et al. 2011, 2015; Klug et al. 2021). The Hangenberg crisis was a

60 global mass extinction event at the Devonian/ Carboniferous boundary (Caplan & Bustin

61 1999; Kaiser et al. 2011), which reflects one of the six largest mass extinction events in

62 earth's history. The Hangenberg crisis followed the Kellwasser event at the Frasnian/

63 Famennian boundary and affected vertebrate groups to an extent that is comparable to

64 the Big Five mass extinctions (McGhee 1996; McGhee et al 2012, 2013). Therefore, it is

65 seen as a bottleneck in vertebrate evolution and the recovery of formerly diverse

66 vertebrate groups (such as some agnathans, sarcopterygians and placoderms) after

67 the event was minimal (Sallan and Coates 2010; Frey et al. 2018). Indeed, the

68 Hangenberg crisis was more severe than formerly thought and caused a larger diversity

69 loss on genus level than the Kellwasser event (Sallan & Coates 2010). The Hangenberg

70 black shale marks the main extinction phase of the event and was laid down during a

71 supposed global transgression linked with widespread anoxia. The anoxia were likely

72 caused by eutrophication that led to global extinctions in numerous invertebrate groups

73 such as algae, sponges, ammonoids, trilobites, brachiopods and bivalves (Algeo &

74 Scheckler 1998; Sallan & Coates 2010; Kaiser et al. 2011, 2015) but also in vertebrate

75 groups like chondrichthyans and placoderms (Kaiser et al. 2011).

76 While remains of the previously mentioned invertebrate groups are quite common in the

77 Hangenberg black shale (Schmidt, 1924; Marynowski et al. 2012; Klug et al. 2016;

78   Zhang et al. 2019), it lacks vertebrate remains, which makes the new Meckel's cartilage

79   a particularly important fossil.

80   The cartilaginous endoskeletons of chondrichthyans are covered by a thin layer of

81   calcified cartilage (Kemp & Westrin 1979; Dean & Summers 2006, Seidel et al. 2016,

82   2020; Maisey et al. 2020). This thin layer typically shows a distinct polygonal pattern,

83   which is caused by the presence of tesserae, namely the tessellated calcified cartilage

84   (Seide et al. 2016, 2020, 2021; Maisey et al. 2020). Such cartilage is characteristic for

85   extant as well as Devonian crown chondrichthyans (elasmobranchs and holocephalans,

86   Long et al. 2015; Maisey 2020) while these polygonal structures tend to be less distinct

87   in acanthodians (a paraphyletic group of stem chondrichthyans, Rücklin et al. 2021),

88   where only subtessellated calcified cartilage or globular calcified cartilage is reported

89   (Dean & Summers 2006; Brazeau & Friedman 2014; Brazeau 2020; Maisey et al.

90   2020). Globular calcified cartilage builds the inner layer of tessellated calcified cartilage

91   and can build the entire hard tissue. If globular calcified cartilage is present on the

92   surface a granular pattern is to be expected (Burrow et al. 2015; Maisey et al. 2020).

93   Subtessellated calcified cartilage shows fissures along the surface, which result in an

94   unorganized pattern. Tessellated calcified cartilage with an outer prismatic layer, in

95   contrast, is well organized and a polygonal pattern is distinct (Maisey et al. 2020; Seidel

96   et al. 2020).

97   Among the cartilaginous remains, jaws are one of the most relevant anatomical

98   structures from an evolutionary perspective. The evolution of jaws, the Meckel's

99   cartilage, is seen as a key innovation of gnathostomes enabling the first gnathostomes

100   to broaden their range of feeding strategies and prey upon a much greater diversity of

101 animals (DeLaurier & Gerhart, 2018; Deakin et al. 2022). These innovations contributed

102 greatly to the radiation of gnathostomes and possibly to the decline of agnathans

103 (Brazeau & Friedman 2015; Hill et al. 2018). Nevertheless, only very few quantitative

104 studies about jaw shapes have been published. For example, Hill et al. (2018)

105 quantified jaw shape in extant and in Palaeozoic fishes (Chondrichthyes, Sarcopterygii,

106 Actinopterygii, Placodermii, Acanthodii) and demonstrated that jaw shape has a greater

107 disparity in extant fish clades than during the early gnathostome radiation (Silurian and

108 Devonian). This is mostly caused by the great morphological disparity among extant

109 actinopterygians (Hill et al. 2018). Deakin et al. (2022) also mentioned an increasing

110 disparity in jaw shape with ongoing evolution but the functional disparity of early

111 vertebrate jaws to be highest very early in jaw evolution and optimized for a predatory

112 function. Anderson et al. 2011 also deals with jaw disparity and the influence of

113 environmental changes such as the Kellwasser event, which does not seem to affect

114 jaw disparity very much.

115 The phylogenetic relations within the chondrichthyan total group are still a widely

116 discussed topic (Hanke & Wilson 2006; Brazeau 2009; Davis et al. 2012; Burrow &

117 Rudkin 2014; Brazeau & Friedman 2015; Brazeau & de Winter 2015; Giles et al 2015;

118 Qiao et al. 2016) and acanthodians were just recently recognized as a paraphyletic

119 goup of stem chondrichthyans (Zhu et al. 2013; Coates et al. 2017; Rücklin et al. 2021).

120 Members of this group show characteristics of both principal clades of living

121 gnathostomes (chondrichthyans and osteichthyans), are covered with scales and are

122 often referred to as "spiny sharks" because of the spines in front of their dorsal, anal

123 and paired fins as evident in most taxa of this group (Miles 1970, 1973; Burrow &

124 Rudkin 2014; Qiao et al. 2016). The relationship between jaw shape and phylogeny

125 remains an elusive question since ecological factors likely influence jaw shape to a

126 great degree as well.

127 Our main aim in this article is, 1) to give a detailed description of this novel find and 2) to

128 determine its possible systematic affiliation. For the latter, we used geometric

129 morphometrics since the Meckel's cartilage was found isolated with no further skeletal

130 parts, teeth or scales associated and is therefore hard to assign to a specific taxon. We

131 applied elliptical Fourier (EFA), principal component (PCA) and hierarchical cluster

132 analyses (HCA) to the new small Meckel's cartilage and 41 more chondrichthyan and

133 acanthodian lower jaws. By this action, a morphospace is created which is informative

134 about the relationship between lower jaw shape and phylogeny.

135

136 **Materials & Methods**

137

138 The specimen PIMUZ A/I 5139 (Fig.1) was found in the Moroccan Anti-Atlas at the

139 locality Madene El Mrakib (N30.73093°, W4.70749°). Permit for fossil collection and

140 export were given by the Ministère de l'Energie, des Mines, de l'Eau et de

141 l'Environnement, Rabat, Morocco. The specimen is stored at the Palaeontological

142 Institute and Museum of Zurich (Switzerland). It was largely exposed, but covered parts

143 were carefully prepared using a thin steel-needle. Photos of the specimen showing its

144 shape, proportions and preservation (Fig. 1) were taken using a Nikon D2X. Colour and

145 contrast were slightly adjusted in Adobe Photoshop (Adobe Inc. 2019). To show the

146 structure of the fossil's surface in more detail, close-ups were taken with a Leica MZ16

147 F microscope (Fig. 1C, D, E) and gently adjusted in colour and contrast as well.

148

149 **Morphometrics**

150 Morphometric techniques together with multivariate and cluster analysis are standard

151 methods to quantify morphology and evaluate groupings or affinities among taxa

152 (Kaesler & Waters 1972; Younker & Ehrlich 1977; Ferrario et al. 1999; Daegling &

153 Jungers 2000). Here, we use morphometric analyses to compare the new isolated

154 Meckel's cartilage to shapes of other lower jaws with known systematic affiliation and

155 find the most similar shape, or group of shapes, to help determine the new Meckel's

156 cartilage taxonomic affinities at least approximately. To carry out the analyses, outlines

157 of 41 lower jaws representing the main stem and crown chondrichthyan orders were

158 drawn based on photographs and illustrations from the literature (App. 1) using the

159 vector-based software Affinity Designer (Affinity 2019). Sampling is constrained by the

160 limited number of well-preserved fossils of Meckel's cartilages. The jaw shapes used in

161 the analysis were chosen based on the quality of preservation and completeness of the

162 Meckel's cartilage as could be seen in the publications. The sampled jaws belong to

163 taxa from different periods and localities and cover a wide range of sizes (App. 2). This

164 broad sampling range (regarding time, locality and size) was used to find general

165 differences in shape between the different groups. All Meckel's cartilage outlines were

166 digitized in TPS software (Rohlf, 2015). Elliptic Fourier Analysis (EFA) was then

167 performed in the Momocs package (Bonhomme et al., 2014) in R (R Development Core

168 Team, 2020) to statistically compare all sampled lower jaw shapes. A total number of 25

169 harmonics were considered, which gather nearly 99% of the cumulative harmonic power

170 (seen as a measure of shape information) and reconstructs actual morphologies with

171   high accuracy. We obtained a virtual morphospace by performing a principal component

172   analysis (PCA, Fig. 2) on the preordination data to plot the main shape variations. To

173   quantify the morphological similarity amongst the studied jaws, a Hierarchical Cluster

174   Analysis (HCA) using the R package 'dendextend' (Galili et al. 2019) was conducted.

175   Phylogenetic signal was assessed using the lambda and K statistic with 1,000 random

176   permutation in the R package 'phytools' (Revell 2012). Additionally, a Mantel test,

177   correlating phenetic (morphological) and phylogenetic distances was performed in order

178   to assess the degree of morphological convergence in our sample. These metrics are

179   expected to show greater decoupling and, consequently, lower correlation where

180   homoplasy occurs. Phenetic distances were calculated as Euclidean distances in the

181   morphospace, considering all PCs. We repeated the tests in a set of 1000 phylogenetic

182   trees that accounted for phylogenetic and stratigraphic uncertainty. The tree topology is

183   based on Klug et al. (ongoing research). Polytomies were randomly resolved 1000

184   times and each resulting tree was calibrated by randomizing the tip age of every

185   species within the chronostratigraphic unit, at age or subperiod rank, where their first

186   appearance occurs, using the R package 'paleotree'.

187
188   **Results**

189
190   **Systematic Palaeontology**

191   Class Chondrichthyes Huxley, 1880

192   Subclass ? Elasmobranchii Bonaparte, 1838

193   Order ? Ctenacanthiformes Glikman, 1964

194

195   The Meckel's cartilage with a total length of 18 mm and a height of up to 6 mm is nearly

196   complete and preserved in lateral view (Fig. 1A). The posterior part is somewhat

197   incomplete in the main plate and entirely missing in the counterpart (Fig. 1A, B, D).

198   While most of the specimen is visibly different from the sediment due to its internal

199   structure and colour, in the posterior part the Meckel's cartilage limits are less clear and

200   the exact borders between fossil and sediment are difficult to determine. The specimen

201   shows a bright grey to white colour and most of it is somewhat brighter than the

202   sediment. In the main fossil plate and in the counterpart, a distinctive polygonal pattern

203   of the calcified cartilage is visible mainly in the posterior part (Fig. 1E$_{1,2}$) while in the

204   middle to anterior part, the specimen is mineralized in a bright colour. The tessellation is

205   not as geometric as in some extant species (Seidel et al. 2020,2021) but the polygons

206   are distinct. In some areas, the borders of the polygonal tesserae are clearly

207   distinguishable by white outlines that most likely represent the intertesseral fibres

208   (Seidel et al. 2016). Even though the tesserae borders are distinct, the corners, as well

209   as the borders in general are rounded and less distinct. Despite the blurriness, the

210   pattern is very similar to the one that can be seen in the crown chondrichthyan

211   *Tristychius arcuatus* (Brazeau & Friedman 2014, fig. 5C, D).

212   The ventral edge of the Meckel's cartilage is gently convexly curved. The ventral ridge is

213   discernible in spite of the compaction, especially in the middle to posterior part. It

214   follows the shape of the outline of the jaw until about 2.5 mm distance from the posterior

215   end when it bends upwards (Fig. 1A). The Meckel's cartilage becomes higher from

216   posteriorly until just before the articulation. It displays one bulge at the thickened

217   anterior end, which is about 4 mm long and might represent the symphysis. This bulge

218   is followed by a shallow depression, which is 3.5 mm long and a shallow bulge of about

219   2.5 mm length. The preservation is insufficient to identify muscle attachments with

220   confidence. We assume that the anterior 9 mm was the tooth-bearing part (dental

221   sulcus) because the concave upper edge anterior to the articulation ends there and it

222   appears like the dorsal side broadens from this point anteriorly. The next depression

223   extends over 7.5 mm and ends at the articulation. Although the specimen is flattened,

224   the retroarticular flange (cf. Long et al. 2015) at the posterior end is still preserved as a

225   knob. The articulation is positioned dorsally in the posterior end of the jaw but

226   unfortunately, the preservation does not allow to determine the exact shape of the

227   articulation and it seems incomplete.

228

229   **Morphometric Analyses**

230   The PCA shows clear separation between the jaws of the two chondrichthyan clades

231   Elasmobranchii and Holocephalii (Fig. 2). PC 1 (59% of variance) is mostly related to

232   changes in jaw thickness with decreasing thickness from negative to positive scores.

233   PC 2 (13% of variance) mainly reflects changes of the jaw curvature (from strongly

234   convex to slightly concave), with a decrease in curvature from negative to positive

235   scores (Fig. 2). PC 3 (6% of variance) mostly describe changes in the curvature of the

236   anterior end of the jaw as well as changes of the roundness of the posteroventral edge

237   of the jaw (Fig. 2). Holocephalan jaws occupy high PC1 scores of about 0.05 to 0.17

238   and positive PC2 scores and show relatively slender and only slightly curved

239   morphologies. Elasmobranch jaws occupy a wider score range with PC1 scores

240   between -0.8 to 0.08 and PC2 scores between 0.07 and 0.10 (Fig. 2). Most of them plot

241   in the centre of the morphospace between PC1 scores of about -0.5 and 0.01 and PC2

242   scores around 0.0. Elasmobranch jaws show greater shape variation than holocephalan

243   jaws, from thick and bulky to relatively slender. Acanthodian jaws occupy PC1 scores

244   from -0.11 to 0.10 and PC2 scores of -0.12 to 0.05 (Fig. 2) and overlap to a large extent

245   with elasmobranch and holocephalan jaws. Acanthodian jaw shapes vary from bulky

246   and curved to slender and straight. The new specimen plots at -0.01/0.025 (PC1/PC2),

247   which is close to the other sampled acanthodians and some elasmobranchs. The new

248   specimen plots closest to the acanthodian taxa *Ischnacanthus sp. and Latviacanthus*

249   *ventspilsensis.* Furthermore, some ctenacanths plot very close: *Dracopristis*

250   *hoffmanorum, Ctenacanthus sp. Heslerodus divergens,* as well as another

251   elasmobranch of the order Synechodontiformes*: Palidiplospinax occultidens* (Fig. 2).

252   In the dendrogram derived from the HCA, the new Hangenberg black shale Meckel's

253   cartilage plots closest to the acanthodian *Latviacanthus ventspilsensis*. The

254   acanthodian *Ischnacanthus sp.* and the elasmobranch of *Heslerodus divergens*

255   constitute sequential sister groups to those two (Fig. 3). Overall, there is not a clear

256   grouping among the three classes (Fig. 3). However, at a lower clustering rank, a

257   separation between holocephalans and elasmobranchs is supported while acanthodians

258   plot together with either elasmobranchs or holocephalans (Fig. 3). We find a significant

259   phylogenetic signal as measured by the metrics K (equal to 0.501 ± 0.071; *p*-value =

260   0.004 ± 0.004) and lambda (equal to 0.995 ± 0.123; *p*-value = 0.0001 ± 0.0001; Fig. 4),

261   but no significant correlation in between phenetic and phylogenetic distances in the

262   Mantel tests (R statistic = -0.045 ± 0.009; *p*-value = 0.632 ± 0.032, all data expressed in

263   mean ± standard deviation, Fig. 5).

264

Discussion

266 Our methodological framework based on EFA, PCA and HCA allows for discriminating

267 holocephalans from elasmobranchs as well as some clades of lower systematic rank,

268 but discrimination of acanthodians as a whole from holocephalans and elasmobranchs

269 is not evident (Figs. 2, 3). We detect a strong phylogenetic signal in our dataset (Fig. 4),

270 altogether suggesting that outline jaw shape by itself can be, to some extent,

271 informative for systematic placement of disarticulated remains and add support to other

272 evidence. However, it has to be kept in mind that our morphometric analysis considers

273 two-dimensional outline shape and, potentially, some relevant anatomical information to

274 discriminate among other groups might not be captured. Further, the lack of correlation

275 between phylogenetic and phenetic distances in Mantel tests (Fig. 5) entail the

276 presence of an important homoplasy, which might hinder the interpretations of

277 phylogenetic affinity from general morphology. Similarities in jaw shape can also result

278 from adaptation. Jaw shape can, for example, be an adaption to a certain lifestyle as in

279 durophagous sharks (Herbert & Motta 2018) or in general be connected to diet in

280 combination with water depth (Motta & Huber 2012). Small variations in shape could

281 also occur due to fossilisation, preparation and errors in redrawing the different outlines,

282 but we do not expect this to have a major effect in our results as preliminary studies

283 have supported that biological signal is still well preserved when minor taphonomical

284 alterations exist (Angielczyk & Sheets 2007).

285 The inclusion of the new Hangenberg black shale jaw in the analysis revealed that it is

286 most similar in shape to lower jaws of certain acanthodian (i.e., *Ischnacanthus sp.* and

287 *Latviacanthus ventspilsensis*) as well as elasmobranchs (the ctenacanths *Dracopristis*

288   *hoffmanorum*, *Ctenacanthus sp.*, and *Heslerodus divergens*; and the synechodontiform

289   *Palidiplospinax occultidens*) (Figs. 2, 3). A holocephalan affinity is unlikely as all

290   considered taxa from this group fall in a separate area of the morphospace. The

291   Hangenberg black shale jaw sits slightly closer to acanthodian jaw shapes than to

292   elasmobranch jaw shapes but whether it is of acanthodian or of elasmobranch origin is

293   difficult to ascertain solely from those analyses and further information is needed to

294   determine its possible origin. An acanthodian origin would entail its inclusion within the

295   paraphyletic groups of stem chondrichthyans (Rücklin et al.2021) while an

296   elasmobranch origin would entail its inclusion in one of the two sister groups of crown

297   chondrichthyans (Elasmobranchii and Holocephali, Maisey et al. 2012).

298   Besides the HBS Meckel's cartilage, the only vertebrate fossils known from the

299   Hangenberg black shale are some poorly preserved chondrichthyan teeth (Klug et al.

300   2016), which are not determined but could be of symmoriiform origin (? *Stethacanthus*,

301   Coates & Sequeira 2001, fig. 5 F-I). However, given out analyses, a holocephalan origin

302   seems unlikely. The exclusion of a holocephalan origin is further supported by the

303   absence of a terminally positioned articulation, which is typical for holocephalans

304   (Coates et al. 2017, character matrix). Due to incomplete preservation of the

305   articulation, it cannot be compared in detail to other chondrichthyan lower jaws.

306   Among the few characters present in the new HBS Meckel's cartilage, some can help to

307   further distinguish its most probable affinity. Thus, the jaw of the ctenacanth *Heslerodus*

308   *divergens* (Hodnett et al. 2021) seems to share some features not directly captured by

309   outline analysis, which are less distinct in both acanthodian jaws that plot close to the

310   HBS jaw. The jaw of *Heslerodus divergens* has a relatively thin anterior to middle part

311   comparable to the first 9 mm of the new jaw that we described as the probable tooth

312   bearing part. Following this, in both jaw shapes, a ridge is present leading to a second

313   depression that ends in the articulation. In the jaw of *Heslerodus divergens,* this shape

314   is more distinct than in the HBS jaw while both acanthodian jaws are dorsally straighter

315   shaped (Fig. 6). Additionally, Hodnett et al. (2021) describes "*a well-developed ventral*

316   *ridge on the lateral margin of the Meckel's cartilage that extends over two thirds the*

317   *length of the jaw(…)"*, as a synapomorphy of ctenacanths. A ventral ridge is one of the

318   few features of the new Hangenberg black shale jaw, which is easily recognized (Fig.

319   1). *Ischnacnathus sp*. shows a ventral ridge as well but when comparing the HBS jaw

320   ventral ridge to the other two, the one of *Heslerodus divergens* is a lot more similar

321   (Fig.6).

322   In addition, a distinct polygonal structure is visible on the surface of the jaw (Fig. 1C).

323   This pattern is characteristic for tessellated calcified cartilage, which is widely accepted

324   as a synapomorphy of extant and extinct crown chondrichthyans (Brazeau & Friedman

325   2014; Long, et al. 2015; Seidel et al. 2016, 2021; Maisey et al. 2020). Tessellated

326   calcified cartilage is made of an inner layer of globular calcified cartilage and an outer

327   layer of prismatic calcified cartilage (Maisey et al 2020). Only the outer prismatic layer

328   shows the typical polygonal pattern while the globular calcified cartilage shows a

329   granular surface (see for example the acanthodian *Climatius reticulatus* in Burrow et al.

330   2015, fig. 1, I).

331   Fossils of the acanthodian group (paraphyletic group of stem chondrichthyans) mostly

332   do not show a polygonal pattern, since no prismatic outer layer is present, but only

333   globular calcified cartilage (Maisey et al. 2020). However, Maisey et al. (2020) describes

334   the presence of subtessellated calcified cartilage in some acanthodians, while actual

335   tessellated calcified cartilage (showing the outer prismatic layer) is apparently absent

336   (Brazeau & Friedman 2014). Acanthodians like *Climatius (Burrow et al. 2015)*,

337   *Ischnacanthus* (Burrow et al. 2018) or *Cheiracanthus* (den Blaauwen 2019) are

338   mentioned to show this subtessellated calcified cartilage. When looking at *Climatius,* it

339   appears granular and no actual polygons are visible on the surface as mentioned above

340   (Burrow et al. 2015, fig. 1, I). In *Ischnacanthus* (Burrow et al. 2018), a subtessellated

341   calcified cartilage is described using histology; we cannot compare the HBS specimen

342   to that. In *Cheiracanthus* (den Blaauwen 2019), the surface appears *"globular or*

343   *randomly tessellated"*. To sum this up, acanthodian fossils, or stem chondrichthyans,

344   show a rather globular or irregular pattern (Burrow et al 2015 fig. 1, I; Long et al. 2015,

345   fig. 9, A), which differs a lot from the regular polygonal pattern in crown

346   chondrichthyans.

347   A polygonal pattern is evident in the new specimen but the borders of the single

348   tesserae are slightly blurred taphonomically, which might have been caused by

349   dissolution of the unmineralized collagen between the tiles (intertesseral fibre; Seidel et

350   al 2016). However, the pattern is distinct and regular, making an elasmobranch origin

351   more likely than an acanthodian origin. In fact, it is as regular as the polygonal pattern in

352   the crown chondrichthyan *Tristychius arcuatus* (Brazeau & Friedman 2014).

353   Based on the results from morphometric analyses and the presence of both a ventral

354   ridge on the lateral margin and tessellated calcified cartilage with a regular polygonal

355   pattern, we assign the new Meckel's cartilage to the order Ctenacanthiformes with some

356   reservations (Fig. 7). To some degree, this classification remains tentative and a bigger

357   sample size could help to test the hypothesis. Further fossil finds as well as a better

358   understanding of the early development of tessellated calcified cartilage in early fishes

359   could help to classify the new jaw in more detail. However, this study presents an

360   important fossil find, filling a gap in the fossil record and provides crucial information

361   about the difficulties of determining the systematic affiliation of isolated cartilaginous

362   fossil remains.

363

364   **Conclusions**

365   The newly described Meckel's cartilage is the first known fossil cartilage remain from

366   the Hangenberg black shale from the Moroccan Anti-Atlas. It is 18 mm in length,

367   ventrally convexly curved and shows a biconcave dorsal edge. PCA and HCA reveal a

368   strong similarity in shape with certain acanthodians and elasmobranchs and a

369   phylogenetic signal is detected in our dataset. We conclude that jaw shape can be

370   informative about the systematic placement of disarticulated skeletal elements but

371   further information is needed since homoplasy is pervasive. The structure of the

372   tessellated calcified cartilage was used as a character for classification. It shows a

373   distinct polygonal pattern which is characteristic for crown chondrichthyans.

374   Furthermore, its general shape as well as the shape of the ventral ridge were compared

375   to two of the jaws that were classified as the most similar by PCA and HCA analyses.

376   This comparison suggests a ctenacanth affiliation. Considering the mentioned evidence,

377   we assigned the new lower jaw to the order Ctenacanthiformes, tentatively.

378

379

Acknowledgements

380

381 We thank the Ministère de l'Energie, des Mines, de l'Eau et de l'Environnement

382 (Direction du Développement Minier, Division du Patrimoine, Rabat, Morocco) for

383 providing working and sample export permits. At an earlier stage, Louis Dudit (Zürich)

384 helped with the Fourier analysis. We showed photos of the Meckel's cartilage to Carole

385 Burrow (Queensland) and Jake Leyhr (Uppsala) and discussed its affiliation. We greatly

386 appreciate their suggestions regarding both the jaw and the teeth from the HBS. We

387 thank the reviewers for XX. HGF is funded by the Generalitat Valenciana

388 (APOSTD/2021/119).

389

References

391 Adobe Inc. 2019: *Adobe Photoshop*, Available at:
392 https://www.adobe.com/products/photoshop.html
393
394 Affinity 2019: *Affinity Designer,* Available at https://affinity.serif.com/en-us/designer/
395
396 Algeo, T. J. and Scheckler, S. E. 1998: Terrestrial-marine teleconnections in the Devonian: links
397 between the evolution of land plants, weathering processes, and marine anoxic events.
398 *Philosophical Transactions of the Royal Society London* B353, 113–130.

399 Anderson, P. S. L.; Friedman, M.; Brazeau, M.; Rayfield, E. J. 2011: Initial radiation of jaws
400 demonstrated stability despite faunal and environmental change. *Nature* 476, 206-209.

401 Andreev, P., Coates, M. I., Karatajūtė-Talimaa, V., Shelton, R. M., Cooper, P. R., Wang, N. Z.,
402 & Sansom, I. J. 2016: The systematics of the Mongolepidida (Chondrichthyes) and the
403 Ordovician origins of the clade. *PeerJ*, *4*, e1850.

404 Angielczyk, K. D. and Sheets, H. D. 2007: Investigation of simulated tectonic deformation in
405 fossils using geometric morphometrics. *Paleobiology* 33, 125–148.

406 Bapst, D. W. 2012: "paleotree: an R package for paleontological and phylogenetic analyses of
407 evolution." *Methods in Ecology and Evolution* 3.5, 803-807.

408 Bonhomme, V.; Picq, S.; Gaucherel, C.; Claude, J. 2014: Momocs: outline analysis using R.
409 *Journal of Statistical Software* 56:1–24.
410 Brazeau, M. D. 2009: The braincase and jaws of a Devonian 'acanthodian' and modern
411 gnathostome origins. *Nature* 457 (7227), 305–308.

412   Brazeau, M. D. 2012: A revision of the anatomy of the Early Devonian jawed vertebrate
413   *Ptomacanthus anglicus* Miles. *Palaeontology* 55 (2), 355–367.

414   Brazeau, M. D.; Friedman, M. 2014: The characters of Palaeozoic jawed vertebrates. *Zoological*
415   *Journal of the Linnean Society* 170 (4), 779–821.

416   Brazeau, M. D.; Giles, S.; Dearden, R. P.; Jerve, A.; Ariunchimeg, Y. A.; Zorig, E. et al. 2020:
417   Endochondral bone in an Early Devonian 'placoderm' from Mongolia. *Nature Ecology and*
418   *Evolution* 4 (11), 1477–1484.

419   Brazeau, M. D. & de Winter, V. 2015: The hyoid arch and braincase anatomy of *Acanthodes*
420   support chondrichthyan affinity of 'acanthodians'. *Proceedings. Biological sciences* 282 (1821),
421   20152210.

422   Brazeau, M. D. & Friedman, M. 2015: The origin and early phylogenetic history of jawed
423   vertebrates. *Nature* 520 (7548), 490–497.

424   Burrow, C. J.; Blaauwen, J. den; Newman, M. 2020: A redescription of the three longest-known
425   species of the acanthodian *Cheiracanthus* from the Middle Devonian of Scotland.
426   *Palaeontologia Electronica* 23(1): a15.

427   Burrow, C. J.; Davidson, R. G.; Den Blaauwen, J. L.; Newman, M. J. 2015: Revision of *Climatius*
428   *reticulatus* Agassiz, 1844 (Acanthodii, Climatiidae), from the Lower Devonian of Scotland, based
429   on new histological and morphological data. *Journal of Vertebrate Paleontology* 35 (3),
430   e913421.

431   Burrow, C. J.; Newman, M.; Blaauwen, J. den; Jones R.; Davidson, R. G. 2018: The Early
432   Devonian ischnacanthiform acanthodian *Ischnacanthus gracilis* (Egerton, 1861) from the
433   Midland Valley of Scotland. *Acta geologica Polonica* 68 (3), 335–362.

434   Burrow, C. J. & Rudkin, D. 2014: Oldest Near-Complete Acanthodian: The First Vertebrate from
435   the Silurian Bertie Formation Konservat-Lagerstätte, Ontario. *Plos One* 9 (8), e104171.

436   Burrow, C. J.; Trinajstic, K.; Long, J. 2012: First acanthodian from the Upper Devonian
437   (Frasnian) Gogo Formation, Western Australia. *Historical Biology* 24 (4), 349–357.

438   Cabrera, D. Alfredo; C., Alberto L.; Cozzuol, M. A. 2012: Tridimensional Angel Shark Jaw
439   elements (Elasmobranchii, Squatinidae) from the Miocene of Southern Argentina. *Ameghiniana*
440   49 (1), 126–131.

441   Caplan, M. L.& Bustin, R. M. 1999: Devonian–Carboniferous Hangenberg mass extinction
442   event, widespread organic-rich mudrock and anoxia: causes and consequences.
443   *Palaeogeography, Palaeoclimatology, Palaeoecology* 148 (4) 187-207.

444   Coates, M. I.; Finarelli, J. A.; Sansom, I. J.; Andreev, P. S.; Criswell, K. E.; Tietjen, K.; Rivers,
445   M. L.; La Riviere, P. J. 2018: An early chondrichthyan and the evolutionary assembly of a shark
446   body plan. *Proceedings. Biological sciences* 285, 20172418, 10 pp.
447   http://dx.doi.org/10.1098/rspb.2017.2418

448   Coates, M. I.; Gess, R. W. 2007: A new reconstruction of *Onychoselache traquairi*, comments
449   on early chondrichthyan pectoral girdles and hybodontiform phylogeny. *Palaeontology* 50 (6),
450   1421–1446.

451   Coates, M. I.; Gess, R. W.; Finarelli, J. A.; Criswell, K. E.; Tietjen, K. 2017: A symmoriiform
452   chondrichthyan braincase and the origin of chimaeroid fishes. *Nature* 541 (7636), 208–211.

Coates, M. I.; Sequeira, S. E. K. 2001: A new stethacanthid chondrichthyan from the lower Carboniferous of Bearsden, Scotland. In *Journal of Vertebrate Paleontology* 21 (3), 438–459.

Coates, M. I.; Tietjen, Kristen; O, Aaron M.; Finarelli, J. A. 2019: High-performance suction feeding in an early elasmobranch. In *Science advances* 5 (9), eaax2742.

Daegling, D. J., & Jungers, W. L. 2000: Elliptical Fourier analysis of symphyseal shape in great ape mandibles. *Journal of Human Evolution*, *39*(1), 107-122.

Davis, S. P.; Finarelli, J. A.; Coates, M. I. 2012: *Acanthodes* and shark-like conditions in the last common ancestor of modern gnathostomes. *Nature* 486 (7402), 247–250.

Deakin, W. J., Anderson, P. S. L., den Boer, W., Smith, T. J., Hill, J., Rücklin, M., Donoghue, P. C. J., Rayfield, E. J. 2022: Increasing morphological disparity and decreasing optimality for jaw speed and strength during the radiation of jawed vertebrates. *Science Advances* 8, eabl3644

Dean M.N. & Summers A.P. 2006. Mineralized cartilage in the skeleton of chondrichthyan fishes. *Zoology* 109, 164–168.

Dearden, R. P.; Giles, S. 2021: Diverse stem-chondrichthyan oral structures and evidence for an independently acquired acanthodid dentition. *Royal Society open science* 8 (11), 210822.

DeLaurier, A. & Gerhart, J. 2018: Evolution and development of the fish jaw skeleton. *Wiley Interdisciplinary Reviews*: *Developmental Biology* 8. 10.1002/wdev.337.

den Blaauwen, J.; Newman, M.; Burrow, C. 2019: A new cheiracanthid acanthodian from the Middle Devonian (Givetian) Orcadian Basin of Scotland and its biostratigraphic and biogeographical significance. *Scottish Journal of Geology* 55, 166-177.

Derycke, C.; Olive, S.; Groessens, E.; Goujet, D. 2015: Paleogeographical and paleoecological constraints on paleozoic vertebrates (chondrichthyans and placoderms) in the Ardenne Massif Shark radiations in the Famennian on both sides of the Palaeotethys. *Palaeogeography, Palaeoclimatology, Palaeoecology* 414, 61–67

Derycke, C.; Spalletta, C.; Perri, M. C., Corradini 2008: Famennian chondrichthyan microremains from Morocco and Sardinia. *Journal of Palaeontology* 82 (5), 984–995.

Dick, J. R. F. 1981: *Diplodoselache woodi* gen. et sp. nov., an early Carboniferous shark from the Midland Valley of Scotland. *Earth and Environmental Science Transactions of The Royal Society of Edinburgh* 72 (2), 99–113.

Ferrario, V. F., Sforza, C., Tartaglia, G. M., Colombo, A., & Serrao, G. 1999: Size and shape of the human first permanent molar: a Fourier analysis of the occlusal and equatorial outlines. *American Journal of Physical Anthropology: The Official Publication of the American Association of Physical Anthropologists*, *108*(3), 281-294.

Finarelli, J. A. & Coates, M. I. 2014: *Chondrenchelys problematica* (Traquair, 1888) redescribed: a Lower Carboniferous, eel-like holocephalan from Scotland. *Earth and Environmental Science Transactions of The Royal Society of Edinburgh* 105 (1), 35–59.

Frey, L., Coates, M. I., Ginter, M., Hairapetian, V., Rücklin, M., Jerjen, I., Klug, C. 2019: The early elasmobranch *Phoebodus*: phylogenetic relationships, ecomorphology, and a new time-scale for shark evolution. *Proceedings of the Royal Society B*, 20191336, 1-11.

493   Frey, L.; Coates, M. I.; Tietjen, K.; Rücklin, M.; Klug, C. 2020: A symmoriiform from the Late
494   Devonian of Morocco demonstrates a derived jaw function in ancient chondrichthyans.
495   *Communications Biology* 3 (1), 681, 1-10.

496   Frey, L.; Rücklin, M.; Korn, D.; Klug, C. 2018: Late Devonian and Early Carboniferous alpha
497   diversity, ecospace occupation, vertebrate assemblages and bio-events of southeastern
498   Morocco. *Palaeogeography Palaeoclimatology Palaeoecology* 496, 1–17.

499   Galili, T.; Benjamini, Y.; Simpson, G.; Jefferis, G.; Gallotta, M.; Renaudie, J.; Hennig, C. 2019:
500   Dendextend: Extending'dendrogram'functionality in R. *R package version* 1.12. 0.

501   Giles, S.; Friedman, M.; Brazeau, M. D. 2015: Osteichthyan-like cranial conditions in an Early
502   Devonian stem gnathostome. *Nature* 520 (7545), 82–85.

503   Ginter, M.; Hairapetian, V.; Klug, C. 2002: Famennian chondrichthyans from the shelves of
504   North Gondwana. *Acta geologica Polonica* 52 (2), 169–215.

505   Ginter, M. & Maisey, J. G. (2007): The braincase and jaws of *Cladodus* from the Lower
506   Carboniferous of Scotland. In *Palaeontology* 50 (2), 305–322. DOI: 10.1111/j.1475-
507   4983.2006.00633.x.

508   Hanke, G. F.; Davis, S. P.; Wilson, M. V. H. 2001: New Species of the Acanthodian Genus
509   Tetanopsyrus from Northern Canada, and Comments on Related Taxa. *Journal of Vertebrate*
510   *Paleontology* 21 (4), 740–753.

511   Hanke, G. F.; Wilson, M. V. H. 2006: Anatomy of the early Devonian acanthodian
512   *Brochoadmones milesi* based on nearly complete body fossils, with comments on the evolution
513   and development of paired fins. *Journal of Vertebrate Paleontology* 26 (3), 526–537.

514   Harris, J. E. 1938: The neurocranium and jaws of *Cladoselache. Scientific publications of the*
515   *cleveland museum of natural history* 1, 1-12.

516   Herbert, A. M. & Motta, P. J. 2018: Biomechanics of the jaw of the durophagous bonnethead
517   shark. *Zoology* 129, 54-58.

518   Hill, J. J.; Puttick, M. N.; Stubbs, T. L.; Rayfield, E. J.; D., Philip C. J. 2018: Evolution of jaw
519   disparity in fishes. *Palaeontology* 61 (6), 847–854.

520   Hodnett, J. P. M.; Grogan, E.; Lund, R.; Lucas, S. G.; Elliott, D. 2021: Ctenacanthiform sharks
521   from the Late Pennsylvanian (Missourian) Tinajas member of the Atrasado formation, central
522   New Mexico: *New Mexico Museum of Natural History and Science Bulletin* 84, 391-424.

523   Johanson, Zerina; Underwood, Charlie; Richter, Martha (Eds.)- 2018: Evolution and
524   Development of Fishes. *Cambridge University Press*.

525   Kaesler, R. L., & Waters, J. A., 1972: Fourier analysis of the ostracode margin. *Geological*
526   *Society of America Bulletin, 83(4), 1169-1178.*

527   Kaiser, S. I.; Aretz, M.; Becker, R. T. 2015: The global Hangenberg Crisis (Devonian–
528   Carboniferous transition): review of a first-order mass extinction. *Geological Society, London,*
529   *Special Publications* 423 (1), 387–437.

530   Kaiser, S. I.; Becker, R. T.; Steuber, T.; Aboussalam, S. Z. 2011: Climate-controlled mass
531   extinctions, facies, and sea-level changes around the Devonian–Carboniferous boundary in the

532 eastern Anti-Atlas (SE Morocco). *Palaeogeography Palaeoclimatology Palaeoecology* 310 (3-4),
533 340–364.

534 Kemp, N. E. &Westrin, S. K. 1979: Ultrastructure of calcified cartilage in the endoskeletal
535 tesserae of sharks. *Journal of morphology* 160 (1), 75–109.

536 Klug, C.; Frey, L.; Korn, D.; Jattiot, R.; Rücklin, M. 2016: The oldest Gondwanan cephalopod
537 mandibles (Hangenberg Black Shale, Late Devonian) and the mid-Palaeozoic rise of jaws.
538 *Palaeontology* 59 (5), 611–629.

539 Klug, C.; Lagnaoui, A.; Jobbins, M.; Bel Haouz, W.; Najih., A. 2021: The swimming trace
540 *Undichna* from the latest Devonian Hangenberg Sandstone equivalent of Morocco. *Swiss
541 Journal of Palaeontology* 140 (1), 19.

542 Klug, S. & Kriwet, J. 2008: A new basal galeomorph shark (Synechodontiformes, Neoselachii)
543 from the Early Jurassic of Europe. *Naturwissenschaften* 95 (5), 443–448.

544 Klug, C., Coates, M., Frey, L., Greif, M., Jobbins, M., Pohle, A., Lagnaoui, A., Bel Haouz, W.,
545 Ginter, M. In prep. Broad snouted cladoselachian with sensory specialisation at the base of
546 modern chondrichthyans.

547 Lane, J. A.& Maisey, J. G. 2012: The visceral skeleton and jaw suspension in the durophagous
548 hybodontid shark *Tribodus limae* from the Lower Cretaceous of Brazil. *Journal of Palaeontology*
549 86 (5), 886–905.

550 Long, J. A.; Burrow, C. J.; Ginter, M.; Maisey, J. G.; Trinajstic, K. M.; Coates, M. I.; Young, G.
551 C.; Senden, T. J. 2015: First shark from the Late Devonian (Frasnian) Gogo Formation, Western
552 Australia sheds new light on the development of tessellated calcified cartilage. *Plos one* 10 (5),
553 e0126066.

554 Luccisano, V.; Pradel, A.; Amiot, R.; Gand, G.; Steyer, J. S.; Cuny, G. 2021: A new *Triodus*
555 shark species (Xenacanthidae, Xenacanthiformes) from the lowermost Permian of France and
556 its paleobiogeographic implications. *Journal of vertebrate Palaeontology* 41 (2), 1-18. DOI:
557 10.1080/02724634.2021.1926470

558 Maisey, J. G. 1985: Cranial morphology of the fossil elasmobranch *Synechodus dubrisiensis.*
559 *American Museum novitates* no. 2804: New York, N.Y.: American Museum of Natural History.

560 Maisey, J. G. 2012: What is an 'elasmobranch'? The impact of palaeontology in understanding
561 elasmobranch phylogeny and evolution. *Journal of Fish Biology* 80, 918-951.

562 Maisey, J. G. 2013: The diversity of tessellated calcification in modern and extinct
563 chondrichthyans. *Revue de Paléobiologie* 32 (2), 355–371.

564 Maisey, J. G., Denton, J. S. S., Burrow, C., Pradel, A. 2020: Architectural and ultrastructural
565 features of tessellated calcified cartilage in modern and extinct chondrichthyan fishes. *Journal of
566 fish biology* 98 (4), 919–941.

567 Maisey, J. G., Janvier, P., Pradel, A., Denton, J. S. S.; Bronson, A.; Miller, R.; Burrow, C. J.
568 2018: *Doliodus* and pucapampellids: Contrasting perspectives on stem chondrichthyan
569 morphology. In Johanson, Z., Underwood, C., Richter, M. (Eds.): Evolution and Development of
570 Fishes. *Cambridge University Press*, 87–109.

571 Marynowski L., Zatoń, M., Rakociński, M., Filipiak, P., Kurkiewicz, S., Pearce, T. J. 2012:
572 Deciphering the upper Famennian Hangenberg Black Shale depositional

573 environments based on multi-proxy record. Palaeogeography, Palaeoclimatology,
574 Palaeoecology 346-347, 66-86.

575 McGhee, G.R., 1996: The Late Devonian Mass Extinction: The Frasnian/Famennian Crisis.
576 *Columbia Universtiy Press, New York.*

577 McGhee, G.R., Sheehan, P.M., Bottjer, D.J., Droser, M.L., 2012: Ecological ranking of
578 Phanerozoic biodiversity crises: the Serpukhovian (Early Carboniferous) crisis had a greater
579 ecological impact than the end-Ordovician. *Geology* 40, 147–150.

580 McGhee, G. R., Clapham, M. E., Sheehan, P. M., Bottjer, D. J., Droser, M. L., 2013. A new
581 ecological-severity ranking of major Phanerozoic biodiversity crises. *Palaeogeography,*
582 *Palaeoclimatology, Palaeoecology* 370, 260–270.

583 Miles, R. S. 1970: Remarks on the vertebral column and caudalfin of acanthodian fishes.
584 *Lethaia* 3, 343–362.
585
586 Miles, R. S. 1973: Articulated acanthodian fishes from the Old Red Sandstone of England, with
587 a review of the structure and evolution of the acanthodian shoulder-girdle. *Bulletin of the British*
588 *Museum (Natural History). Geology* 24, 111–213.
589
590 Motta, P. J., Huber, D. R. 2012: Prey capture behavior and feeding mechanics of
591 elasmobranchs. In: Carrier, J. C., Musick, J. A., Heithaus, M. R. (Eds.), Biology of Sharks
592 and Their Relatives. *CRC Press, Boca Raton, FL* pp. 153–209.

593 Qiao, T.; King, B.; Long, J. A.; Ahlberg, P. E.; Zhu, M. 2016: Early Gnathostome Phylogeny
594 Revisited: Multiple Method Consensus. *Plos one* 11 (9), e0163157.

595 R Development Core Team. 2020: R: A Language and Environment for Statistical Computing. *R*
596 *Foundation for Statistical Computing,* Vienna, Austria, pp.

597 Revell, L. J. 2012: Phytools: An R package for phylogenetic comparative biology (and other
598 things). *Methods in ecology and evolution (2), 217-223.*

599 Rieppel, O. 1981: The hybodontiform sharks from the Middle Triassic of Monte San Giorgio,
600 Switzerland. *Neues Jahrbuch für Geologie und Paläontologie* 161 (3), 324 - 353.

601 Rohlf, F. J. 2015: The tps series of software. *Hystrix, the Italian Journal of Mammalogy* 26:9–12.

602 Romano, C. & Brinkmann, W. 2010: A new specimen of the hybodont shark *Palaeobates polaris*
603 with three-dimensionally preserved Meckel's cartilage from the Smithian (Early Triassic) of
604 Spitsbergen. *Journal of Vertebrate Paleontology* 30 (6), 1673–1683.

605 Rücklin, M.; King, B.; Cunningham, J. A.; Johanson, Z.; Marone, F.; Donoghue, P. C. J. 2021:
606 Acanthodian dental development and the origin of gnathostome dentitions. *Nature Ecology and*
607 *Evolution* 5 (7), 919–926.

608 Sallan, L. C. & Coates, M. I. 2010: End-Devonian extinction and a bottleneck in the early
609 evolution of modern jawed vertebrates. *Proceedings of the National Academy of Sciences of the*
610 *United States of America* 107 (22), 10131–10135.

611 Schmidt, H. 1924: Zwei Cephalopodenfaunen an der Devon-Carbongrenze im Sauerland.
612 Jahrbuch der Preußischen Geologischen Landesanstalt 44 (for 1923), 98–171.
613 Schultze, H. P.; Zidek, N. J. 1982: Ein primitiver acanthodier (pisces) aus dem Unterdevon
614 Lettlands. *Paläontologische Zeitschrift* 56 (1-2), 95–105.

615 Seidel R, Blumer M, Chaumel J, Amini S, Dean M.N. 2020. Endoskeletal mineralization in
616 chimaera and a comparative guide to tessellated cartilage in chondrichthyan fishes (sharks,
617 rays and chimaera). *Journal of the Royal Society Interface*. 17 (171), 20200474.

618 Seidel, R.; Jayasankar, A. K.; Dean, M. N. 2021: The multiscale architecture of tessellated
619 cartilage and its relation to function. *Journal of fish biology* 98 (4), 942–955.

620 Seidel, R.; Lyons, K.; Blumer, M.; Zaslansky, P.; Fratzl, P.; Weaver, J. C.; Dean, M. N. 2016:
621 Ultrastructural and developmental features of the tessellated endoskeleton of elasmobranchs
622 (sharks and rays). *Journal of anatomy* 229 (5), 681–702.

623 Wilga; C. D. & Motta, P. J. 1998: Conservation and variation in the feeding mechanism of the
624 spiny dogfish squalus acanthias. *The Journal of experimental biology* 201 (9), 1345–1358.

625 Younker, J. L., & Ehrlich, R. 1977: Fourier biometrics: harmonic amplitudes as multivariate
626 shape descriptors. *Systematic Biology, 26(3), 336-342.*

627 Zangerl, R.; Case, G. R. 1976: Cobelodus aculeatus (Cope) an anacanthous shark from
628 Pennsylvanian Black Shales of North America. *Palaeontographica, Sonder Abdruck* 154, 107–
629 157.

630 Zhang, M., Becker, R. T., Ma, X., Zhang, Y., Zong, P. 2019: Hangenberg Black Shale with
631 cymaclymeniid ammonoids in the terminal Devonian of South China. Palaeobiodiversity and
632 Palaeoenvironments 99: 129-142.

633

634 Zhu, M.; Yu, X.; Ahlberg, P. E.; Choo, B.; Lu, J.; Qiao, T. et al. 2013: A Silurian placoderm with
635 osteichthyan-like marginal jaw bones. *Nature* 502 (7470), 188–193.

Figure 1

Meckel's cartilage outlines and close ups

Meckel's cartilage of a ctenacanth chondrichthyan from the Hangenberg black shale, Madene El Mrakib; PIMUZ A/I 5139. A, lateral view; B_1, traced outline and ventral ridge; B_2, counterpart with outline; C, Close up of the anterior area; D, close up of the posterior area; $E_{1,2}$, Close-up photos of the cartilage showing the polygonal pattern. Abbreviations: sym - symphysis, ma - muscle attachment area, vr - ventral ridge, re.fl - retroarticular flange. Scale bar for A, $B_{1,2}$ equals 5 mm. Scale bar for C, D, $E_{1,2}$ equals 1 mm. Arrow indicates Anterior (A) and Posterior (P).
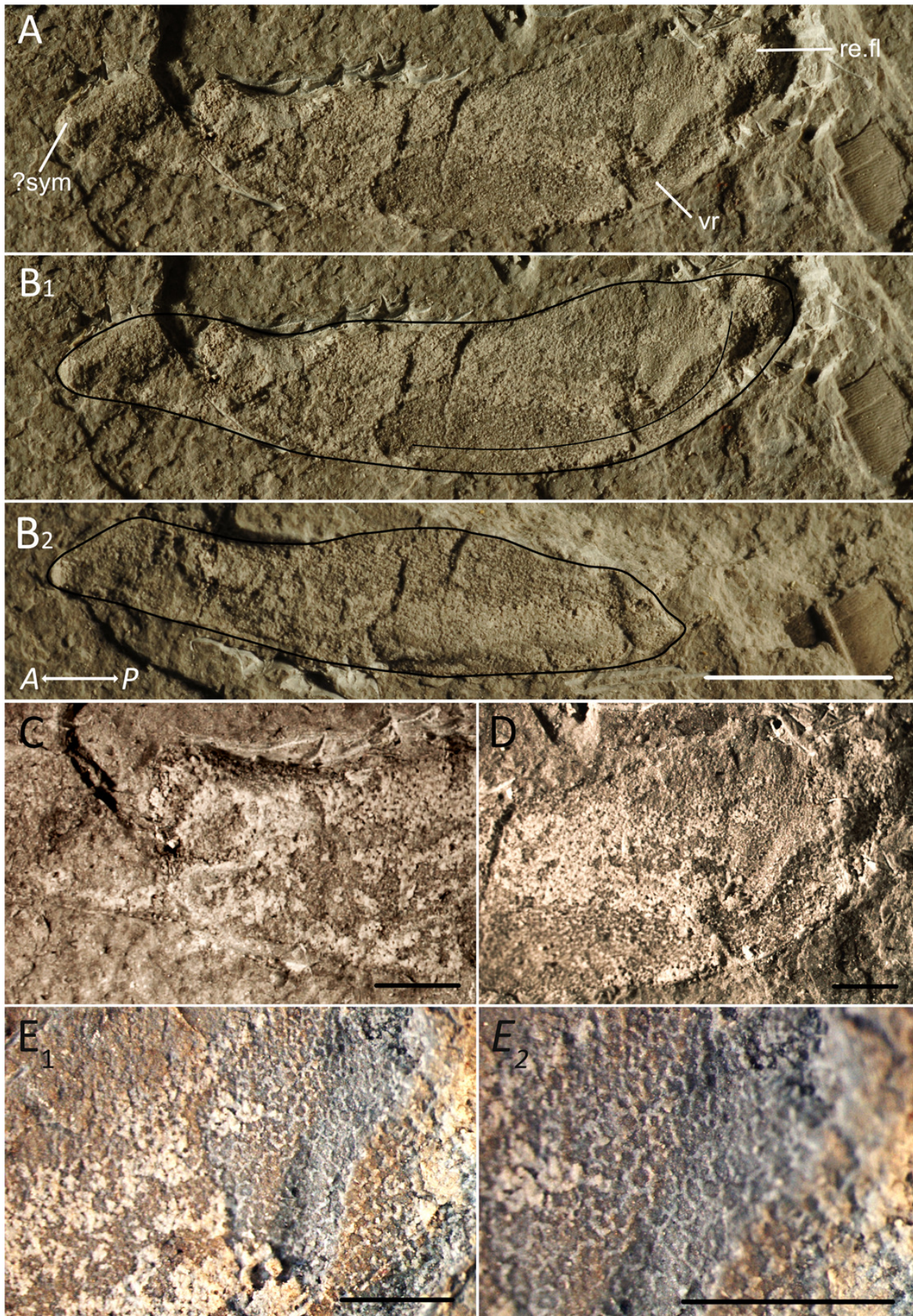
Figure 2

PCA and morphospace with all sampled lower jaws

Principal Component Analysis of some fossil and recent chondrichthyan lower jaws. Orange colours: acanthodians; purple colours: holocephalan; blue colours: elasmobranchs. The new lower jaw from the Hangenberg black shale is represented by a black dot and grey colours represent lower jaws of unknown class and order. A jaw morphospace is represented in the background showing the shape variation. The new Hangenberg black shale jaw plots close to jaws of acanthodians as well as elasmobranchs. Lv: Latviacanthus ventspilsensis, Is: Ischnacanthus *sp*., Po: Palidiplospinax occultidens, Dh: Dracopristis hoffmanorum, Ct: Ctenacanthus *sp*. Hd: Heslerodus divergens.
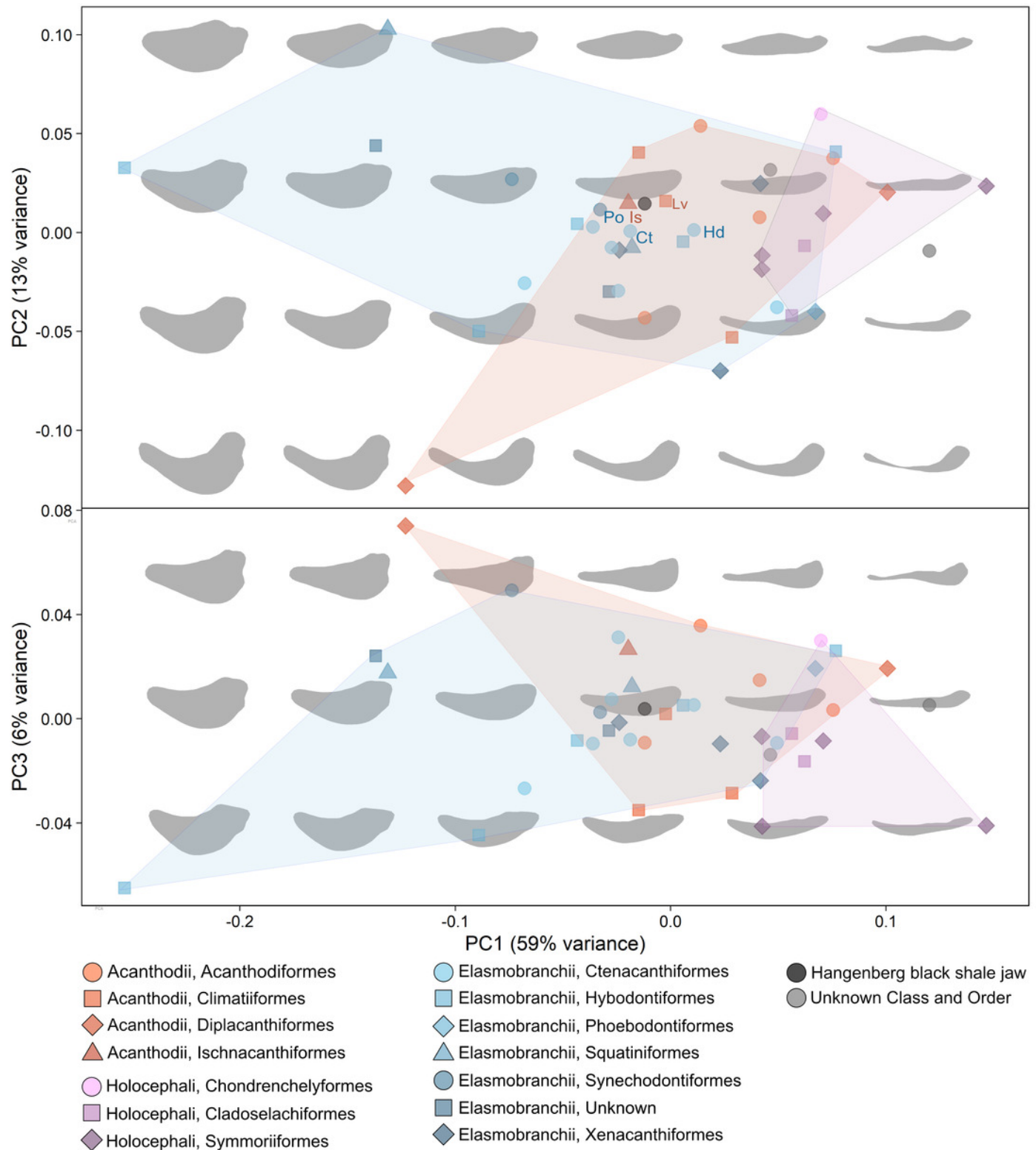
Figure 3

Dendrogram showing morphological distances of the sampled lower jaws

Dendrogram showing morphological distances regarding the first principal components from the PCA. Orange colours: acanthodians; purple colours: holocephalan; blue colours: elasmobranchs. The elasmobranchs plot mainly on the top, while holocephalan jaws plot mainly at the bottom. Acanthodian jaws are scattered over the whole dendrogram. The lower jaw from the Hangenberg black shale is closest to some acanthodian jaws such as that of Ischnacanthus sp.

Morphological distance
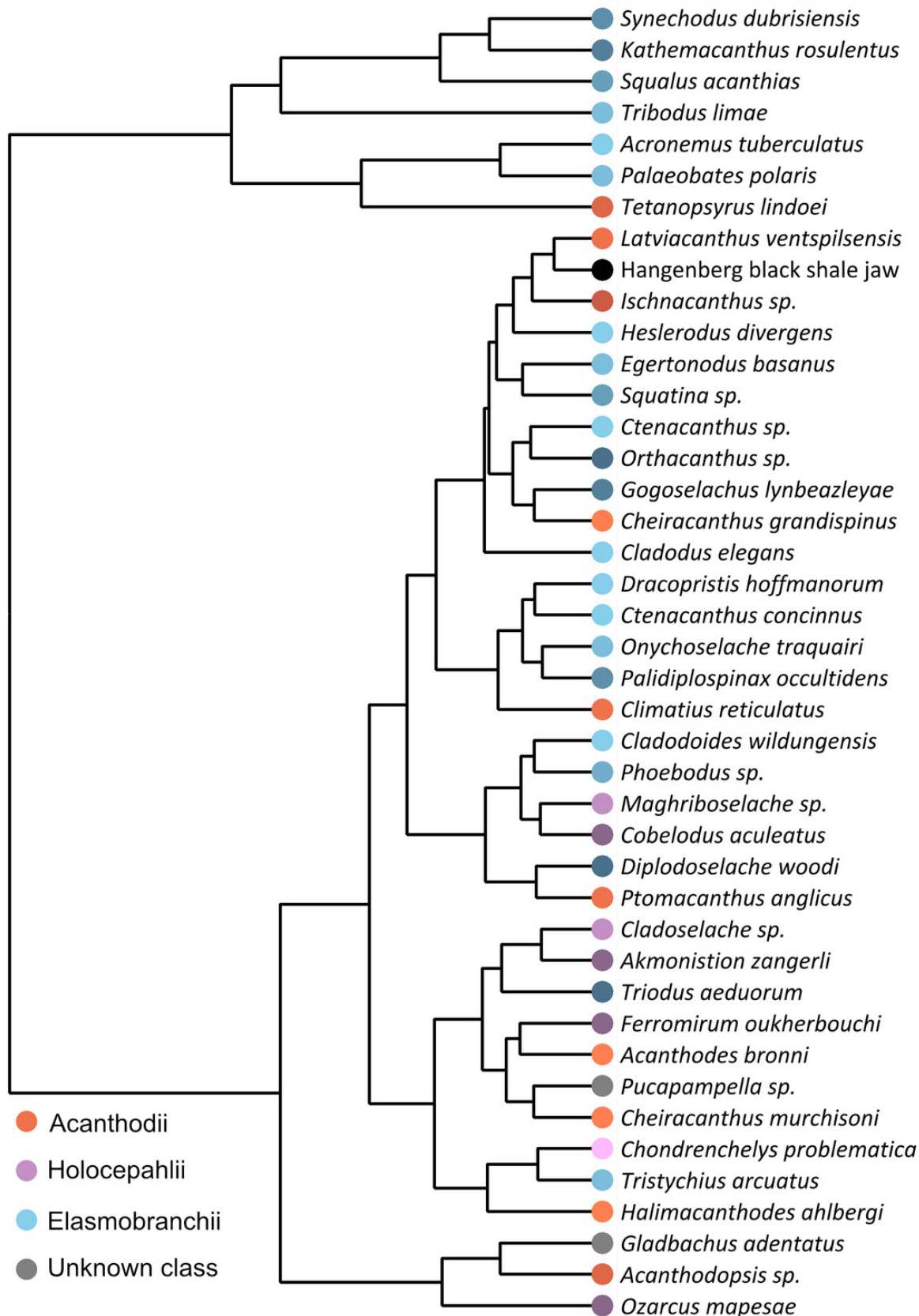
Figure 4

Phylogenetic signal metrics and tests of significance

Phylogenetic signal metrics and tests of significance performed in 1000 trees accounting for phylogenetic and stratigraphic uncertainty.
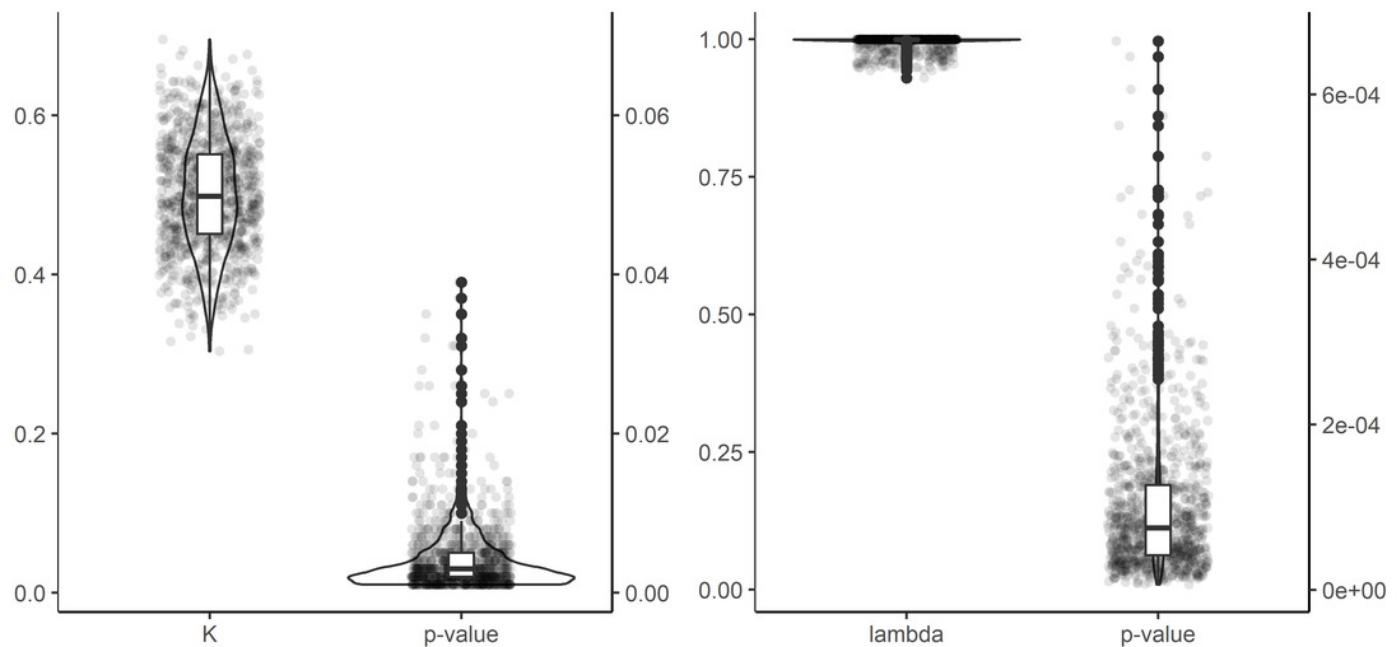
Figure 5

Mantel test results

Mantel test analysis performed in 1000 trees accounting for phylogenetic and stratigraphic uncertainty. R statistic values close to 1 or -1 support strong correlation between phylogenetic and phenetic distances, while values close to 0 support weak correlation.
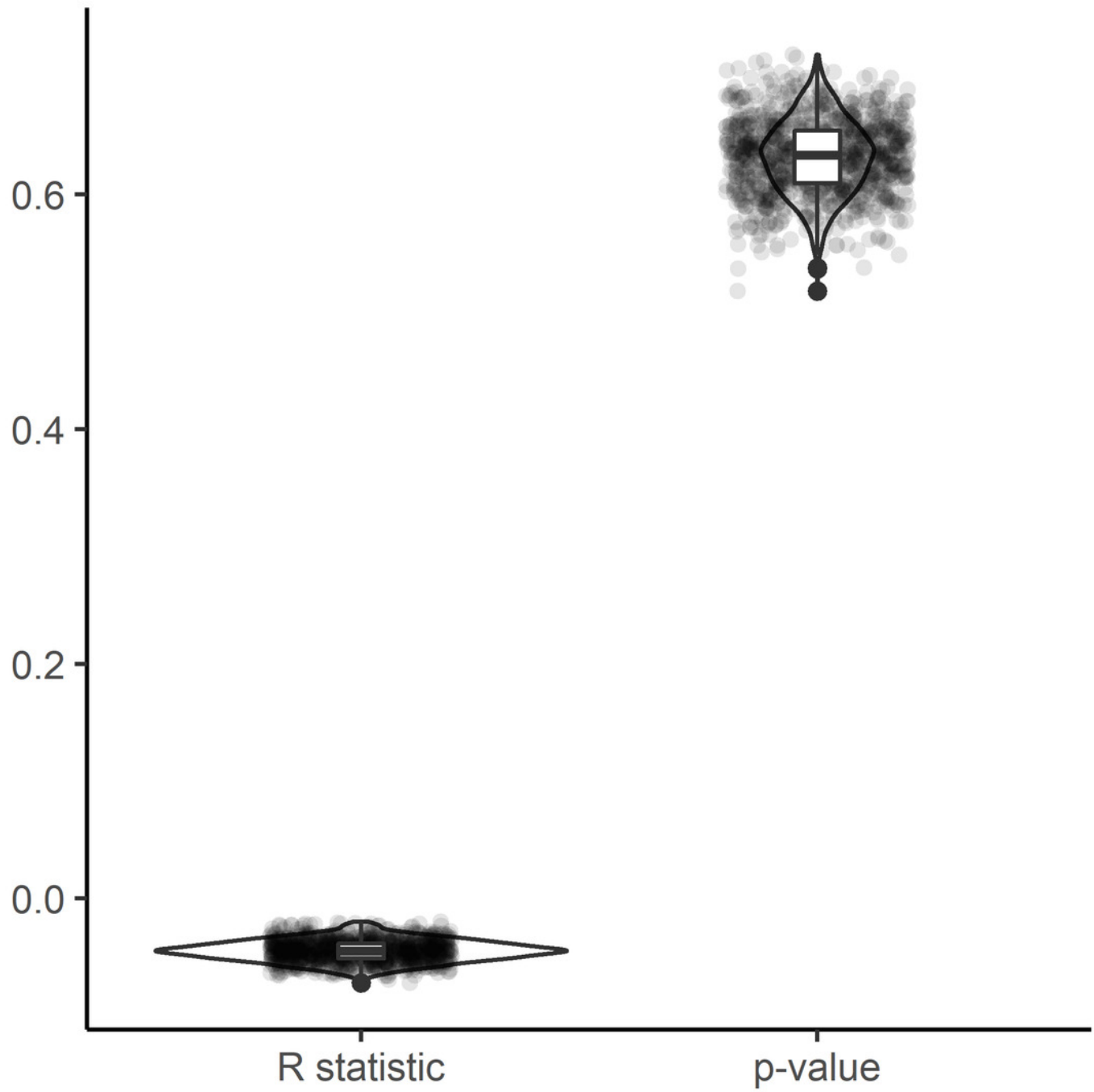
Figure 6

visual jaw shape comparison

Direct comparison of the new HBS Meckel's cartilage (grey, top) with the two most similar jaw shapes of two different groups (pink, middle) and an overlay of both (pink and grey, bottom). A: the elasmobranch Heslerodus divergens. B: the acanthodian Ischnacanthus sp. Different characteristic points, that were not captured by the PCA directly, as well as the ventral ridge are compared and both shapes are shown in overlap with the HBS Meckel's cartilage.
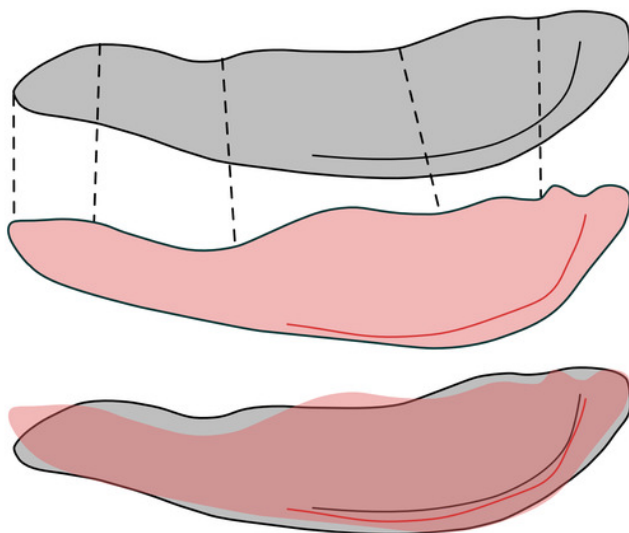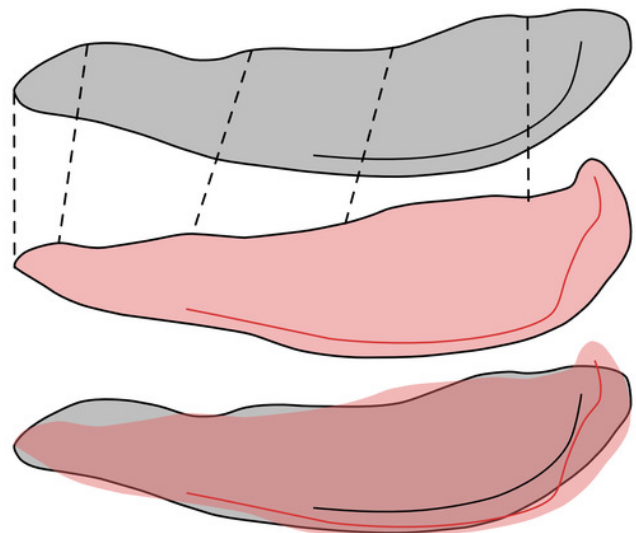
Figure 7

All sampled outlines in a phylogenetic tree showing the possible position of the new Meckel's cartilage

Simplified chondrichthyan phylogeny modified after Klug et al. (in prep.). The lower jaw from the Hangenberg black shale is figured together with the taxa used in the Fourier Analysis. The shapes of the lower jaws were redrawn from the literature (App. 1). The new HBS jaw is suggested to be of ctenacanthiform origin regarding the analyses and comparison of characters.

Xenacanthiformes

Triodus aeduorum *Diplodoselache woodi* *Orthacanthus sp.*

Ctenacanthiformes

Cladodus elegans *Dracopristis hoffmanorum* *Ctenacanthus sp.*

?

Hangenberg black shale jaw

Ctenacanthus concinnus *Heslerodus divergens* *Acronemus tuberculatus*

Phoebodontiformes

Phoebodus sp.

Synechodontiformes

Synchodus dubrisiensis *Palidiplospinax occultidens*

Squaliformes

Squalus acanthias *Squatina sp.*

Hybodontiformes

Tristychius arcuatus *Palaeobates polaris* *Egertonodus basanus* *Onychoselache traquairi* *Tribodus limae*

Gogoselachus lynbeazleyae

Cladodoides wildungensis

Symmoriiformes

Ferromirum sp. *Cobelodus aculeatus* *Akmonistion zangerli* *Ozarcus mapesae*

Cladoselachiformes

Maghriboselache sp. Cladoselache sp.

Chondrenchelyformes

Chondrenchelys problematica

Gladbachus adentatus *Pucapampella sp.*

Kathemacanthus rosulentus

Acanthodiiformes

Acanthodes bronni *Halimacanthodes ahlbergi* *Cheiracanthus murchisoni* *Cheiracanthus grandispinus*

Ischnacanthiformes

Ischnacanthus sp.

Diplacanthiformes

Tetanopsyrus lindoei *Acanthodopsis sp.*

Latviacanthus ventspilsensis

Climatiiformes

Ptomacanthus anglicus *Climatius reticulatus*